Catalysis Letters 32 (1995) 281–291

Effect of the addition of alkali metals on the metallic phase of Pt / Al_2O_3 catalysts

Sergio R. de Miguel, Alberto A. Castro, Osvaldo A. Scelza
Instituto de Investigaciones en Catálisis y Petroquímica – INCAPE
(Facultad de Ingeniería Química, Universidad Nacional del Litoral – CONICET),
Santiago del Estero 2654, 3000 Santa Fe, Argentina

and

Javier Soria
Instituto de Catálisis y Petróleoquímica, Campus Universidad Autónoma,
Cantoblanco, 28049 Madrid, Spain

Received 24 August 1994; accepted 6 March 1995

The effect of the addition of alkali metals to Pt / Al_2O_3 catalysts for dehydrogenation of paraffins was studied. Results can be interpreted in terms of different effects. Thus, the addition of alkali metals produces a poisoning of the acid sites of the alumina support and a modification of the characteristics of the metallic phase. The latter effect involves not only an increase of the Pt particles size, but also an electronic modification of the metallic phase. These two effects are more marked with alkali metals with higher ionic radius, such as K.

Keywords: supported metallic catalysts for paraffins dehydrogenation; effect of alkali metals addition; characterization of catalysts

1. Introduction

Platinum and platinum-containing bimetallic catalysts supported on alumina are widely used for naphtha reforming, and for dehydrogenation of heavy linear alkanes ($C_{10}-C_{15}$) in the petrochemical industries. However, this kind of catalysts has lately also been used for dehydrogenation of light paraffins [1–3]. The difference between dehydrogenation and reforming catalysts lies mainly on the acidity of the support. Reactions which are catalyzed by the acid sites of the support (such as isomerization, cracking and polymerization) must be inhibited in order to increase the yield to olefins in dehydrogenation processes. The acid sites of the alumina can be poisoned by adding alkali metal ions during the preparation of these catalysts [4]. However, the alkali metal addition could affect not only the acidic function of the support but also the characteristics of the metallic phase. In this way, Mross et al. [5] found that alkali metal cations improved the activity and selectivity of transition metal catalysts for CO hydrogenation, thus modifying the electronic properties of the catalyst surface. Moreover, the addition of potassium to iron [6], ruthenium [7] or nickel [8] increased the selectivity toward olefins. Additionally, Park et al. [9,10] found that the K addition to Pd/Al_2O_3 improved the activity and selectivity to ethylene in the hydrogenation of acetylene. They explained this effect in terms of the more basic nature of K-doped alumina, which produces an electron transfer from K to Pd, thus resulting in a higher Pd electron density. Figoli et al. [11] studied the selective hydrogenation of styrene over Pd/Al_2O_3 and found changes in the electronic state of Pd, by XPS measurements, when sodium was added to the support.

In this paper we study the influence of the addition of alkali metals on the behavior of the acidic and the metallic function of Pt/Al_2O_3 catalysts by using different characterization techniques, such as the determination of H_2PtCl_6 adsorption isotherms on pure and doped alumina, H_2 chemisorption measurements, TEM, FTIR, TPR, XPS and test reactions. Additionally, the modification of the catalytic properties as a consequence of the alkali metal addition was determined by catalytic tests in the propane dehydrogenation reaction.

2. Experimental

A commercial γ-Al_2O_3 (CK-300 from Cyanamid Ketjen) was used as a support. The alumina support (35–80 mesh) was previously calcined in air at 923 K during 3 h. Samples of Li(0.3 wt%)/Al_2O_3 and K(1.69 wt%)/Al_2O_3 were prepared by impregnation of Al_2O_3 with $LiNO_3$ and KOH aqueous solution, respectively; then they were dried at 393 K and finally calcined in an air stream at 773 K. Pt(0.3 wt%)/Al_2O_3–alkali metal catalysts were prepared by two different impregnation sequences. In the first one, alumina was impregnated with an aqueous solution of $LiNO_3$ or KOH, dried at 393 K and then impregnated with a H_2PtCl_6 aqueous solution (samples denoted as Li (or K),Pt/Al_2O_3). In the second procedure, alumina was impregnated in an inverse sequence (samples denoted as Pt,Li (or K)/Al_2O_3). After impregnation, samples were dried at 393 K, calcined in an air stream at 773 K and reduced in H_2 at the same temperature. The alkali metal concentration in the catalysts was 0.43 mmol g^{-1} (equivalent to 0.3 wt% of Li or 1.69 wt% of K). Besides, a Pt(0.3 wt%)/Al_2O_3 catalyst was also prepared by impregnation of alumina with H_2PtCl_6 aqueous solution.

The physical properties of the pure and doped Al_2O_3 (previously evacuated at 773 K for 15 h) were determined in a volumetric equipment Micromeritics ASAP 2000.

The adsorption isotherms of H_2PtCl_6(aq.) on pure and doped alumina were determined at 298 K by shaking 0.5 g of the support with 5 ml of a H_2PtCl_6 aqueous solution of a given concentration. The initial concentration of the chloroplatinic acid solution ranged between 0.3 and 7.5 mg Pt ml^{-1}. After reaching the equilibrium (24 h), the liquid and solid phases were separated and the Pt content in each phase was determined by atomic absorption spectrometry.

Transmission electron microscopy (TEM) images were taken on a Jeol Jem-2000 FX microscope fitted with X-ray fluorescence (EDXS). They were recorded using a 200 kV accelerating voltage and a direct magnification of 600000×. Catalyst samples, previously reduced in H_2 at 773 K, were ground into a fine powder, ultrasonically dispersed in isopropanol and finally dropped onto a copper grid, where the solvent was evaporated.

Hydrogen chemisorption measurements were determined by a H_2 pulse technique at room temperature in a Micromeritics Pulse Chemisorb 2700 equipment. Before chemisorption, samples were reduced in H_2 at 773 K and then cooled down to room temperature in a helium stream.

Temperature programmed reduction (TPR) experiments were carried out in a conventional TCD system by using 10 ml min^{-1} of a H_2(5%v)–N_2 gaseous mixture, and a constant heating rate of 6 K min^{-1}. Before TPR, samples were calcined in situ with dry air at 773 K.

FTIR spectra were taken on a Nicolet 5ZDX spectrometer. All the samples, in the form of compressed self-supporting disks of 25 mg cm^{-2}, were previously reduced in H_2 at 773 K and evacuated (under a residual pressure of 10^{-5} Torr) at 723 K during 50 min. Spectra were recorded after adsorbing 30 Torr of CO at 298 K. The background spectrum corresponding to CO gas and the cell windows was subtracted in all the cases. In order to determine the spectra at low CO coverages, samples were submitted to successive outgassing treatments (10^{-5} Torr) at increasing temperatures (up to 600 K) until the total disappearance of the linear Pt–CO band. The CO coverages were calculated as the ratio between the integrated area of the linear band after evacuation at a given temperature and that corresponding to the adsorption at 298 K without further evacuation.

X-ray photoelectron spectroscopy (XPS) spectra were recorded on a Fisions Escalab 200 R spectrometer. Catalysts were previously outgassed and then reduced at 773 K under a H_2 atmosphere in the pretreatment chamber.

Catalysts were tested in the propane dehydrogenation reaction at 853 K in a differential reactor, using a space velocity of 0.067 mol propane h^{-1} g cat.$^{-1}$, a sample weight of 200 mg, and a He/propane molar ratio = 9. Previously, samples were reduced in H_2 at 853 K. After reaction, the coke content of the catalysts was determined by microgravimetric measurements (with a Cahn Electrobalance) during temperature programmed oxidation (TPO) experiments up to 1073 K.

The catalytic activity for cyclohexane dehydrogenation (CHD) and for cyclopentane hydrogenolysis (CPH) was determined under atmospheric pressure in a differential flow reactor. CHD was carried out at 573 K by using a H_2/CH molar ratio of 26 and a CH volumetric flow of 6 ml min^{-1}. Reaction conditions for CPH were: $T = 623$ K, H_2/CP molar ratio = 22.5 and CP volumetric flow = 6 ml

Table 1
Surface area (S_{BET}), pore volume (V_g) and average pore diameter (D_p) of pure and alkali-metal doped γ-Al_2O_3

Sample	S_{BET} ($m^2 g^{-1}$)	V_g ($cm^3 g^{-1}$)	D_p (Å)
γ-Al_2O_3	194	0.51	81
Li(0.3 wt%)/Al_2O_3	190	0.49	82
K(1.69 wt%)/Al_2O_3	179	0.47	83

min^{-1}. Before reaction, catalysts were reduced in H_2 at 773 K. The effluent of the reactor was analyzed by gas chromatography.

3. Results

Table 1 shows the values of surface area, pore volume and average pore size for pure and doped alumina. It can be observed that the physical characteristics of the support slightly changed after Li or K addition.

Fig. 1 shows the adsorption isotherms of H_2PtCl_6 on the different supports (γ-Al_2O_3, Li(0.3 wt%)/Al_2O_3 and K(1.69 wt%)/Al_2O_3). These adsorption isotherms were fitted by the Langmuir equation,

$$C_S = KLC_L/(1 + KC_L), \quad (1)$$

where C_S and C_L are the equilibrium concentrations of Pt in the solid and the liquid, respectively, K is the adsorption equilibrium constant of Pt and L is the saturation concentration of Pt in the solid. From the linearized form of the adsorption isotherms,

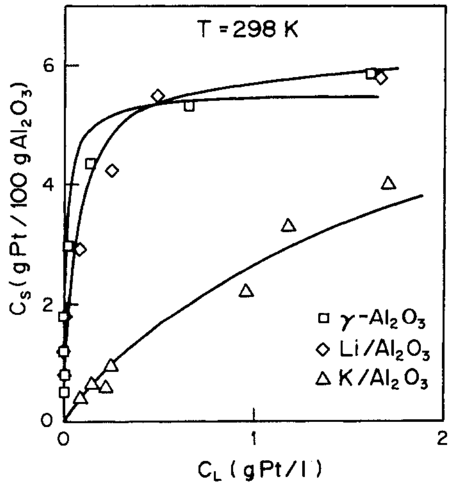

Fig. 1. Adsorption isotherms of H_2PtCl_6(aq.) on Al_2O_3, Li(0.3 wt%)/Al_2O_3 and K(1.69 wt%)/Al_2O_3. Solid lines correspond to isotherms calculated with the parameters reported in table 2.

$$1/C_S = 1/L + (1/KL)(1/C_L), \tag{2}$$

K and L values were calculated and they are shown in table 2. It can be observed that the saturation concentration of Pt (L) is very similar for all the supports. On the other hand, the high value of the adsorption equilibrium constant (K) of Pt on pure γ-Al_2O_3 indicates a strong interaction of the metallic precursor with the alumina surface. This parameter for pure alumina is nine times higher than that for Li(0.3 wt%)/Al_2O_3, and 185 times higher than that for K(1.69 wt%)/Al_2O_3. These results clearly indicate a weaker Pt adsorption on the alumina doped with alkali metals, mainly with those of higher ionic radius, such as K.

The different supported Pt catalysts were characterized by transmission electron microscopy (TEM). Micrographs showed that Pt/Al_2O_3, Pt,Li/Al_2O_3 and Li,Pt/Al_2O_3 catalysts displayed similar Pt particle sizes, while catalysts doped with K showed larger particle sizes. It must be noted that the diffuse contour of the particles hindered an exact measurement of the metallic particle sizes.

Table 3 shows the values of chemisorbed H_2 (H) for the Pt catalysts supported on pure and doped alumina. It is observed that the alkali metal addition to Pt/Al_2O_3 modifies the chemisorptive characteristics of the metallic phase. In this way, Li-doped Pt/Al_2O_3 catalysts showed a small decrease of the H value with respect to that of Pt/Al_2O_3. However, this decrease was more pronounced for K-doped Pt/Al_2O_3 catalysts. In this sense, the amount of hydrogen chemisorbed on the K,Pt/Al_2O_3 catalyst was approximately one half of the value corresponding to the catalyst without alkali metals. Besides, table 3 shows that the H_2 chemisorption capacities in samples prepared impregnating first with the alkali metals and then with Pt are 15–20% lower than those corresponding to samples prepared by using the inverse impregnation sequence.

Fig. 2 shows TPR profiles of the different Pt catalysts. The Pt/Al_2O_3 sample displayed a main peak with the maximum at 533 K and a broad reduction zone at higher temperatures (which finishes at 773 K). The TPR profiles of both Li-doped Pt/Al_2O_3 catalysts were very similar to that of Pt/Al_2O_3. However, K-doped Pt/Al_2O_3 catalysts showed that the maximum of the main peak is shifted to a lower temperature with respect to that of the undoped sample (20–35 K). This shift could be explained either by an electronic modification of Pt due to K addition or by an effect derived from the higher Pt particle sizes in the K-doped samples. It must be

Table 2
K and L values of the Langmuir equation for the adsorption of H_2PtCl_6(aq.) on pure and doped Al_2O_3

Support	K (ml/mol Pt)	L (mol Pt/g)
γ-Al_2O_3	3.41×10^7	2.83×10^{-4}
Li(0.3 wt%)/Al_2O_3	3.79×10^6	3.15×10^{-4}
K(1.69 wt%)/Al_2O_3	1.84×10^5	2.56×10^{-4}

Table 3
Values of the H_2 chemisorption (H) and integrated areas of the bands corresponding to the linear chemisorption of CO on Pt sites (I_{Pt-CO}) and on Lewis sites of γ-Al_2O_3 ($I_{CO-Lewis}$), respectively, for the different catalysts

Catalyst	H (ml H_2 g^{-1})	I_{CO-Pt} (a.u. cm^{-1})	$I_{CO-Lewis}$ (a.u. cm^{-1})
Pt/Al_2O_3	0.065	4.58	0.40
Pt,Li/Al_2O_3	0.055	4.16	0.27
Li,Pt/Al_2O_3	0.046	4.07	0.23
Pt,K/Al_2O_3	0.037	2.70	0.15
K,Pt/Al_2O_3	0.028	2.29	0.15

noted that McCabe et al. [12] found that highly dispersed Pt/Al_2O_3 samples were more difficult to reduce than low-dispersion samples.

Fig. 3 represents IR spectra of CO adsorbed (without further evacuation) at 298 K on the different Pt catalysts. Three different absorption bands were observed for the Pt/Al_2O_3 sample (spectrum a): one band at 2203 cm^{-1}, which is characteristic of CO molecules coordinated with tetrahedrally coordinated Lewis Al^{3+} sites of the alumina surface [13], a second band at 2075 cm^{-1}, which corresponds to the linear form of CO adsorption on Pt, and a small band at 1826 cm^{-1}, which can be assigned to CO adsorbed on two-fold hollow sites of Pt [14]. The band corresponding to CO adsorbed on the Lewis acid sites of the γ-Al_2O_3 was easily removed by evacuation at room temperature. On the other hand, the intensities of the other bands slightly changed, which indicates that after evacuation at 298 K, CO remained adsorbed only on the Pt particles, both in linear and bridge forms. IR

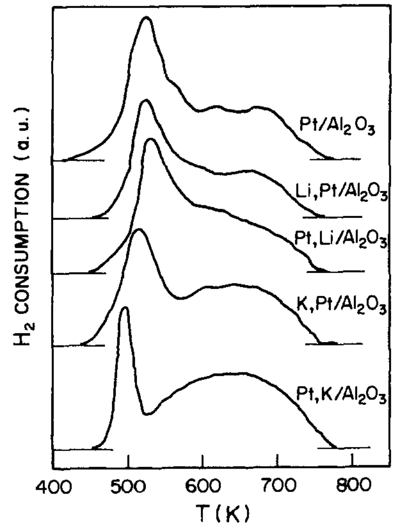

Fig. 2. Temperature programmed reduction (TPR) profiles of the different catalysts.

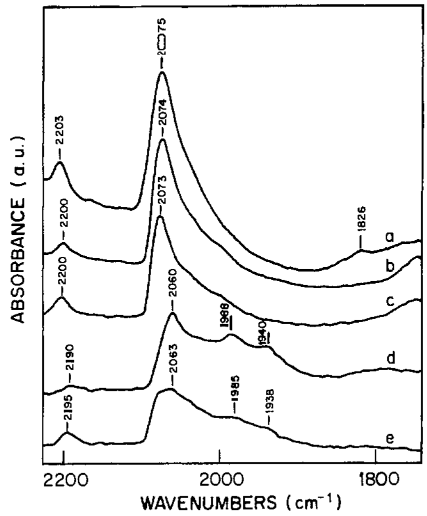

Fig. 3. FTIR spectra of CO adsorbed on different catalysts at 298 K (without further outgassings). (a) Pt/Al_2O_3, (b) Pt,Li/Al_2O_3, (c) Li,Pt/Al_2O_3, (d) Pt,K/Al_2O_3, and (e) K,Pt/Al_2O_3. Spectrum e is magnified.

spectra of Pt/Al_2O_3 catalysts doped with Li (spectra b and c) are very similar and they show the band at 2200 cm^{-1} (with a lower intensity), and that corresponding to the Pt–CO linear adsorption, but slightly shifted to lower frequencies (2073–2074 cm^{-1}). On the other hand, IR spectra of both K-doped Pt/Al_2O_3 samples (spectra d and e) are also very similar and they display a very small band at 2190–2194 cm^{-1} corresponding to CO adsorbed on the Lewis acid sites of the alumina, and a broad band with the maximum at 2060–2063 cm^{-1} in the zone corresponding to the Pt–CO linear adsorption. Besides, these two spectra also show two small bands at 1985–1988 and 1938–1940 cm^{-1}, respectively. It must be noted that no bridge-bonded CO species were observed in Li- or K-doped Pt/Al_2O_3 catalysts.

The integrated area of the IR band corresponding to Lewis acid sites of the alumina decreases for catalysts doped with alkali metals, mainly with K, as shown in table 3. This fact can be due to a blocking effect of the tetrahedrally coordinated Al^{3+} sites of the γ-Al_2O_3 by potassium, as we reported in a previous paper [13]. The area corresponding to the Pt–CO linear band decreases in the following sequence: Pt/Al_2O_3 > Pt,Li/Al_2O_3 > Li,Pt/Al_2O_3 > Pt,K/Al_2O_3 > K,Pt/Al_2O_3. K-doped Pt/Al_2O_3 catalysts (mainly that prepared with an initial impregnation of K and then with Pt) show the lowest integrated area of the IR band corresponding to the Pt–CO linear adsorption. These results indicate that the addition of alkali metals, mainly K, decreases the CO chemisorption capacity. A similar behaviour was found for the H_2 chemisorption, as shown in table 3.

Fig. 4 shows that the linear Pt–CO band is shifted to lower wavenumbers as CO coverage (θ_{CO}) is decreased by successive outgassings at increasing temperatures. This effect was also reported in the literature [15,16]. At low CO coverages,

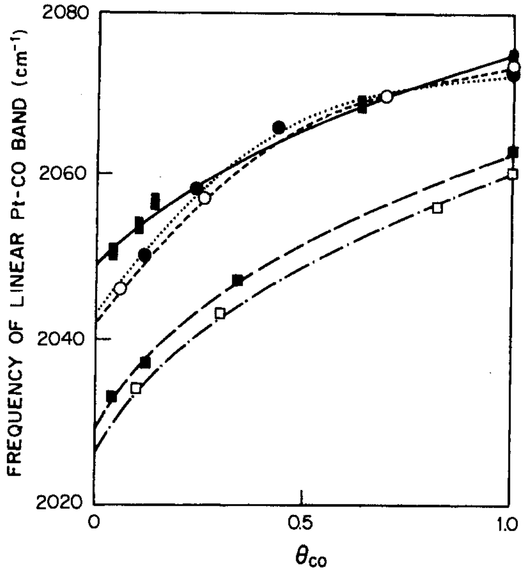

Fig. 4. Frequency of linear Pt–CO band vs. CO coverage. (▮) Pt/Al_2O_3, (○) Pt,Li/Al_2O_3, (●) Li,Pt/Al_2O_3, (□) Pt,K/Al_2O_3, and (■) K,Pt/Al_2O_3.

the stronger adsorption metallic sites can be characterized. Thus, from the extrapolation of the different curves to $\theta_{CO} = 0$, the CO singleton vibration frequencies were obtained. The shift of the carbonyl position, after addition of alkali metals to Pt, can reveal changes in the electronic properties of Pt. In the case of the Li-doped Pt/Al_2O_3 catalysts, the singleton frequencies were very similar for both samples (2042–2043 cm^{-1}) and close to that corresponding to Pt/Al_2O_3 catalyst (2049 cm^{-1}). However, in the case of both K-doped Pt/Al_2O_3 samples, it was found that the CO singleton vibration frequencies markedly fall to 2026–2030 cm^{-1}.

Table 4 shows the propane conversion and the selectivity to propylene of the different catalysts in the propane dehydrogenation reaction at 853 K. Two kinds of reaction products were obtained: (a) propylene (from propane dehydrogenation), (b) methane, ethane and ethylene (from propane cracking and hydrogenolysis).

Table 4

Values of initial conversion (X_0), selectivity to propylene (S) and deactivation rate ($\Delta = X_0 - X_f/X_0$; X_f: propane conversion after 2 h of reaction) and coke content after 2 h of propane dehydrogenation reaction at 853 K

Catalyst	X_0	S (%)	$\Delta = (X_0 - X_f/X_0) \times 100$	Coke (wt%)
Pt/Al_2O_3	5.2	58	27.4	1.25
Pt,Li/Al_2O_3	4.7	55	17.0	0.94
Li,Pt/Al_2O_3	4.3	54	9.0	0.77
Pt,K/Al_2O_3	4.0	52	8.2	0.68
K,Pt/Al_2O_3	4.3	50	7.2	0.22

This table shows a slight decrease both in the initial propane conversion (X_0) and in the selectivity (S) to propylene according to the following sequence: $Pt/Al_2O_3 > Pt,Li/Al_2O_3 > Li,Pt/Al_2O_3 > Pt,K/Al_2O_3 > K,Pt/Al_2O_3$. However, the alkali metal addition to the Pt/Al_2O_3 catalyst produces an important decrease in the deactivation rate (Δ) (see table 4) and in the coke formation (after 2 h of reaction) with respect to the undoped one. This effect is more pronounced for the $K,Pt/Al_2O_3$ catalyst. As it can be observed in table 4, the deactivation rate is parallel with the amount of deposited coke, which means that this carbon deposition is one of the main reasons for the catalytic deactivation.

In order to explain these results, cyclohexane dehydrogenation (CHD) and cyclopentane hydrogenolysis (CPH) rates were measured. TON values for both reactions are indicated in table 5. It can be observed that Pt/Al_2O_3 and $Li,Pt/Al_2O_3$ samples display similar TON values for each reaction. However, the $K,Pt/Al_2O_3$ catalyst shows a lower TON value for CHD reaction, and a higher TON value for CPH reaction, with respect to the undoped sample. Furthermore, the ratio between TON values of CHD and that of CPH for Pt/Al_2O_3 is similar to the one corresponding to $Li,Pt/Al_2O_3$ sample, but is 4.5 times greater than that of the $K,Pt/Al_2O_3$ catalyst. Hence, K addition to Pt improves its hydrogenolytic capacity. This effect can be due to the large metallic particles in the K-doped Pt/Al_2O_3 catalysts, since it is known that big ensembles are required by the hydrogenolysis reaction. The alkali metal addition to Pt not only modifies the metallic function, but also inhibits the strong acidity of the support and hence its cracking capacity. In consequence, the final result of these two opposite effects is a slight decrease of the propane selectivity to propylene in the $K,Pt/Al_2O_3$ catalyst with respect to the undoped one.

On the other hand, coke formation is also favoured by large metallic ensembles. However, our results of propane dehydrogenation showed a low coke deposition on K-doped samples. These apparent opposite effects are discussed below.

Results of X-ray photoelectron spectroscopy (XPS) measurements are shown in table 5. An important shift of the binding energy value of the Pt $4d_{5/2}$ level from 314.2 eV (for Pt/Al_2O_3) to 315 eV (for $K,Pt/Al_2O_3$) was observed.

4. Discussion

The above-mentioned results (adsorption isotherms, H_2 and CO chemisorption

Table 5
Initial TON values for cyclohexane dehydrogenation (TON_{CHD}) at 573 K and for cyclopentane hydrogenolysis (TON_{CPH}) at 623 K, and the binding energy of Pt $4d_{5/2}$ for the different catalysts

Catalyst	TON_{CHD}	TON_{CPH}	BE (eV)
Pt/Al_2O_3	212.9	28.6	314.2
$Li,Pt/Al_2O_3$	209.9	30.8	–
$K,Pt/Al_2O_3$	93.5	56.5	315

and TEM) would indicate that the initial addition of alkali metals to alumina plays an important role in the Pt characteristics, since Li or K adsorption on alumina decreases the Pt adsorption on the stronger adsorption sites of the support, leading to catalysts with lower dispersions and hence with larger Pt crystallites. On the other hand, when the impregnation sequence is Pt, dried and then Li or K, the catalysts also show lower dispersions than that of Pt/Al_2O_3, but higher than those obtained by the inverse impregnation sequence (alkali metal, dried, Pt). Furthermore, the important shifts to lower temperatures of the Pt reduction peak (in TPR experiments) would also indicate the increase of metallic particles in K-doped Pt/Al_2O_3 catalysts.

It has been reported in the literature that the frequency of the stretching vibration of the Pt–CO linear band increases with the Pt particle size [17,18]. However, our FTIR results at $\theta_{CO} = 1$ show a modification of the linear Pt–CO band to lower frequencies in catalysts doped with Li or K, which indicates that other effects, besides the particle size, are modifying the metallic function. The important decrease observed for the CO singleton vibration frequency at $\theta_{CO} = 0$ (fig. 4), for K-doped Pt/Al_2O_3 catalysts, could be due to an electronic modification of the Pt centres. This decrease is more pronounced in catalysts doped with K than with Li. In this way, if an electron transfer from the alkali metal to Pt is occurring, when going from Li to K the ionization potential decreases, and consequently, the corresponding Pt–CO frequency is expected to decrease [19,20]. Other results reported in this paper are in agreement with this hypothesis. Thus, (i) the appearance of new Pt–CO bands between 2000 and 1900 cm^{-1} in the catalysts with K, (ii) the shift of the binding energy value of the Pt $4d_{5/2}$ level when K was added to Pt/Al_2O_3, (iii) the decrease of the TON values for CH dehydrogenation (a structure-insensitive reaction) and (iv) the lower coke formation of Pt/Al_2O_3–alkali metal catalysts (in the propane dehydrogenation reaction), are additional evidence of the electronic modifications of Pt due to the alkali metal.

These electronic effects of the alkali metals on Pt could be produced through modifications of the support properties which induce a change in the metal–support interaction. This hypothesis was also postulated by Park et al. [10] for Pd/Al_2O_3–K catalysts. Our FTIR results showed that the tetrahedral Lewis Al^{3+} sites of alumina are blocked by the alkali metals [13]. Hence, it is probable that the support properties change from acidic to more basic ones, leading to an electron transfer from the modified support to Pt. This effect could produce a lower adsorption strength of the coke precursors on the metallic surface, with beneficial effects on the deactivation and coke formation on Pt. The lower deactivation rate of alkali metal-doped Pt/Al_2O_3 catalysts can also be due to the poisoning effect of alkali metals, mainly K, on the acid sites of the alumina surface. Then, the polymerization reactions of the dehydrogenated products to coke precursors on the acid sites of the support can be inhibited by the alkali metal addition. Additionally, some authors found that the working life of Ni–aluminum oxide catalysts was improved by the addition of small quantities of alkali [21]. In this case, the alkali suppressed the deposition of the so-called kinetic coke on the catalyst.

In conclusion, the effect of addition of alkali metals to Pt supported catalysts produces not only an increase of the Pt particle sizes, but also electronic modifications, giving rise to an electron enrichment of the metallic phase. These two effects are more marked with alkali metals with higher ionic radius, such as K.

Acknowledgement

This work was supported by a grant from CONICET, Argentina. We thank Dr. R.X. Valenzuela for her contribution to the dehydrogenation experiments.

References

[1] I.B. Yarusov, E.V. Zatolokina, N.V. Shitova, A.S. Belyi and N.M. Ostrovskii, Catal. Today 13 (1992) 655.
[2] L.C. Loc, N.A. Gaidai, S.L. Kiperman, *Proc. 9th Int. Congr. on Catalysis*, Calgary, Vol. 3 (1988) 1261.
[3] Eur. Patent Application 0328507 A1 (1989).
[4] G. García Cortez, S.R. de Miguel, O.A. Scelza and A.A. Castro, J. Chem. Technol. Biotechnol. 53 (1992) 177.
[5] W.D. Mross, Catal. Rev. Sci. Eng. 25 (1983) 591.
[6] D.L. King and J.B. Peri, J. Catal. 79 (1983) 164.
[7] T. Okuhara, H. Tamura and M. Misono, J. Catal. 95 (1985) 41.
[8] H. Praliaud, J.A. Dalmon, C. Mirodatos and G.A. Martin, J. Catal. 97 (1986) 344.
[9] Y.H. Park and G.L. Price, J. Chem. Soc. Chem. Commun. (1991) 1188.
[10] Y.H. Park and G.L. Price, Ind. Eng. Chem. Res. 32 (1992) 469.
[11] N. Figoli and P. L'Argentiere, Catal. Today 5 (1989) 403.
[12] R.W. McCabe, C. Wong and H.S. Woo, J. Catal. 114 (1988) 354.
[13] S.R. de Miguel, O.A. Scelza, A.A. Castro and J. Soria, Topics in Catalysis 1 (1994) 87.
[14] D. Haaland, Surf. Sci. 185 (1987) 1.
[15] N. Cant and R. Donaldson, J. Catal. 78 (1982) 461.
[16] D. Haaland and F. Williams, J. Catal. 76 (1982) 450.
[17] R.A. Della Betta, J. Phys Chem. 79 (1975) 2519.
[18] A.A. Solomennikov, Yu.A. Lokhov, A.A. Davydov and Yu.A. Ryndin, Kinet. Katal. 20 (1979) 714.
[19] G. Ertl, D. Prigge, R. Schloegl and M. Weiss, J. Catal. 70 (1983) 379.
[20] D.L. King and J.B. Peri, J. Catal. 79 (1983) 164.
[21] British Gas, DAS 2,634,541, 29 September 1975.